Recent Progress in Phosphorescent Green Emitters

Ying Hou, Jing Wang, Huiqing Pang, Wei Cai, Zheng Wang, Hongbo Li, Zhen Wang, Raymond Kwong, Sean Xia

Summer Sprout Technology Co., Ltd. Beijing, China

Abstract

The fast expansion of AMOLED displays calls for higher brightness, lower power consumption, longer operating lifetime, and wider color gamut. As one of the essential materials in the OLED stack, green phosphorescent emitter plays a key roll in the device performance advancement. Since the first adoption of green phosphorescence in an AMOLED display, great strides have been made on improving the efficiency, lifetime, and line shape. However, further advancement of AMOLED displays require better materials. In this paper, we report on a series of new green emitters recently developed by us to address the issues currently associated with the material. Green emitters developed for P3, Adobe, and BT2020 color gamut will be discussed. We have demonstrated that by employing innovative molecular design, we are able to address the key challenges such as narrow spectra, wide color gamut, and low capacitance, providing a comprehensive solution for the next-generation OLED applications, ranging from mobile devices to augmented and virtual reality systems.

Author Keywords

Green phosphorescent emitters; EL spectra; FWHM; shoulder peak intensity; High efficiency; Low capacitance; HOMO; Hole-electron transport; Optical simulation; Wide color gamut; Adobe, BT2020.

1. Introduction

Organic light emitting devices (OLEDs) have gained widespread adoption in commercial electronic products, including mobile phones, tablets, and AR/VR goggles.[1-2] Nevertheless, the display industry continues to seek performance improvements, such as higher efficiency, longer lifetime, more saturated color, and lower pixel capacitance. High-end displays are also expanding their color gamut, from conventional DCI-P3 to Adobe and even to BT2020. The CIE color coordinates of Adobe and BT2020 green are (0.210, 0.710) and (0.177, 0.797) respectively, the latter is particularly challenging to achieve based on current commercial phosphors.[6] Low capacitance is desired to ensure a quick signal response and high refresh rate, especially at low gray scale scenarios, which is highly desired in high quality displays.[7-9] This is a particular problem for green light emitting materials, which have the highest capacitance of all three colors. Improving all these parameters in a single molecule, however, is an extreme challenge. Both luminous efficiency and color purity can be improved by using emitters with narrower spectra, even without improving the EQE.[3] Most commercial phosphorescent materials, however, exhibit a typical FWHM > 40 nm, limiting their capability to achieve maximum efficiency and high color purity.[4-5] In this paper, we describe the development of phosphorescent emitters with narrow line shapes and low capacitance. Through the study of our emitter families, we discovered that though the capacitance-voltage (CV) behavior of an OLED stack depends on many factors, specialized-designed green emitters alone can have a great positive impact.

We started from optical simulations to prove that narrowing the emission spectrum and reducing the shoulder peak intensity contribute to improved efficiency in top-emission devices. Based on SS GD1, our previously commercialized emitter, we designed SS GD2 with a narrower FWHM and reduced shoulder peak intensity. Compared to SS GD1, the luminous efficiency of SS GD2 increased by 12%, while the CIE (x,y) coordinates shifted from (0.248, 0.725) to (0.215, 0.747). In order to reduce the device capacitance, we studied how it varies with the energy levels and transport properties of the emitter used. Based on these findings, we created SS GD3, which features a shallower HOMO energy level and more balanced hole-electron transport. The accumulated charges in a device made of SS GD3 is successfully reduced by more than half compared to SS GD2. Based on these observations, both capacitance and efficiency can be optimized through the design and modification of molecular structures. These approaches also offer valuable insights for developing high-performance wide-color-gamut OLED emitters.

2. Experiments and results

EL Spectra and Device Performance

To investigate the impact of the emitter spectrum on the efficiency of top-emission devices, we conducted a series of optical simulations. First, the photoluminescence (PL) spectrum of a typical phosphorescent emitter (a) was de-convolved into a main peak (peak 1) and a shoulder peak (peak 2), as illustrated in Figure 1(a). Two new spectra (b and c, respectively) were created by reducing the intensity of peak 2 to 85% and 70% of its original value, then adding them to peak 1 to create the spectra shown in Figure 1(b). Table 1 lists the properties of the spectra a-c.

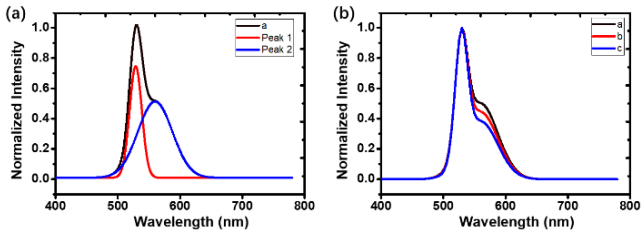

Figure 1. (a) Deconvolution of the emission spectrum "a" into the main peak (peak 1) and shoulder peak (peak 2), and (b) reconstructed emission spectra with reduced shoulder peak intensity (spectra b and c), along with the original spectra a.

These spectra were then incorporated into Setfos 5.1 for optical simulations. The device structure of the top-emission device used in the simulation is shown in Figure 2, where the thickness of the electron blocking layer (EBL) was in the range of 500-700 nm to achieve the maximum efficiency at a particular chromaticity. For all the materials used, 400 Å thick films were deposited on silicon wafers and optical data such as refractive index (n) and extinction coefficient (k) were measured using an ellipsometer. Electrode data were provided by the software default data base. Three spectra a-c were used as the spectrum of the emissive layer (EML) in order to

ISSN 0097-996X/25/5602-1193-$1.00 © 2025

simulate the device performance of a top-emission OLED. The same PL efficiency was set so that the simulation results were only influenced by the spectral characteristics.

Table 1. Basic spectral properties and simulation results (chromaticity and current efficiency) of spectra a–c and of top-emission OLEDS simulated from these spectra. Shoulder peak refers to the intensity of the shoulder peak compared to the main peak.

Spectrum	λ_{max} (nm)	FWHM (nm)	Shoulder peak (%)	CIE	Eff. (cd/A)
a	529	45.2	51	(0.245,0.729)	100%
b	529	32.4	45	(0.232,0.739)	102%
c	529	29.6	38	(0.221,0.748)	106%

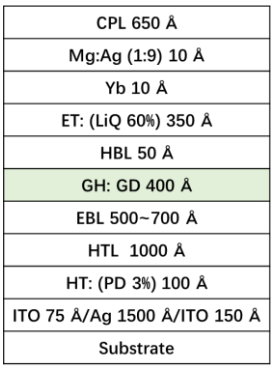

Figure 2. Device structure of a top-emission green OLED used in the simulation.

Table 1 summarizes the simulation results of CIE coordinates and current efficiency of top-emission OLEDS using spectra a–c for the emissive molecule. Reducing the shoulder peak intensity results in a blue shift of the chromaticity in top-emission devices. Typically, a blue shift in chromaticity is associated with a reduction in efficiency for green devices. However, in this case, the efficiency improved owing to the reduction of the shoulder peak. This phenomenon can be attributed to the microcavity effect in top-emission OLEDs, where a narrower spectrum with a reduced shoulder peak results in less energy loss of non-resonant light, thereby enhancing efficiency.

Our commercialized SS GD1 shows a high EQE of 24.3% in a bottom-emission device. However, due to its relatively wide FWHM of 51.5 nm, the maximum current efficiency of a top-emission device is 175 cd/A. In order to increase this efficiency, we designed a new phosphorescent green emitter, SS GD2. The spectra of both GDs are shown in Figure 3, while λ_{max}, FWHM and shoulder peak intensity percentage are listed in Table 2. SS GD2 is not only blue shifted from SS GD1 by 2 nm to a peak of 527 nm, but also has a significantly reduced FWHM of only 33.5 nm. Furthermore, the shoulder peak intensity of SS GD2 drops to only 42% of the main peak.

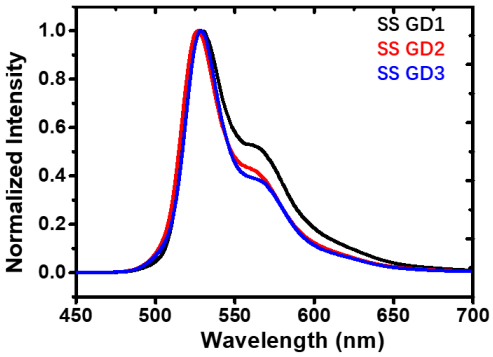

Figure 3. EL spectra of SS GDs1-3 in bottom-emission devices.

Table 2. Comparison of EL spectral properties (λmax, FWHM, and shoulder peak intensity) and EQE for SS GDs1-3.

Spectrum	λ_{max} (nm)	FWHM (nm)	Shoulder peak(%)	EQE(%) @J10
SS GD1	529	51.5	53	24.3
SS GD2	527	33.5	42	25.4
SS GD3	528	31.3	38	27.0

Top-emission devices were fabricated using SS GD1 and 2, according to the device structure shown in Figure 2. The optoelectronic characteristics of all devices were measured at normal incidence using Konica Minolta 2000 with a Keithley 2400 power supply. The operating voltage and current efficiency (CE) were measured at normal incidence at 10 mA/cm^2 and a lifetime to 95% of initial brightness (LT_{95}) of devices were measured at 80 mA/cm^2 at room temperature and using an acceleration factor of 1.8 for extrapolation.

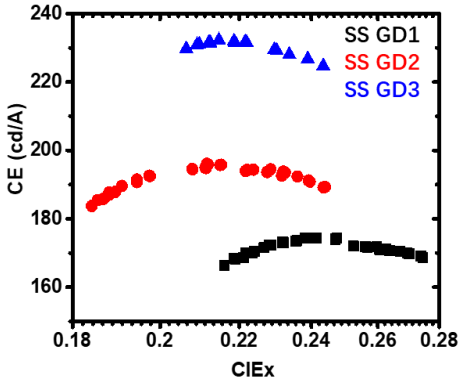

Figure 4. The CE vs. CIE x curve of top-emission OLEDs that use SS GDs1-3

Table 3 summarizes the device performance of top-emission green OLEDs using SS GD1-2 in the emitter layer. The CIE coordinates of SS GD2 are blue-shifted to (0.215, 0.747), and the CE of SS GD2 in top-emission devices reached 196 cd/A, a 12% enhancement over that of SS GD1. Table 2 lists the EQE of SS GD1 and SS GD2 in bottom-emission devices. Figure 4 shows the current efficiency (CE) as a function of CIE x for top-emission OLEDs using SS GD1-2 with different microcavity lengths. The

maximum current efficiency of SS GD2 is not only significantly higher than that of SS GD1, but it is also blue-shifted. These results demonstrate that we successfully engineered the molecular structure of GD to achieve a narrower spectral line shape.

Table 3. Device performance of top-emission green OLEDs using SS GDs at a current density of 10 mA/cm^2

GD	CIE	Voltage (V)	Eff. (cd/A)	Eff ratio	EQE ratio	LT_{95} (h)
SS GD1	(0.248, 0.725)	3.6	175	--	--	2,000
SS GD2	(0.215, 0.747)	3.8	196	1.12	1.05	1,600
SS GD3	(0.220, 0.745)	4.0	230	1.31	1.11	1,400

Capacitance of Devices Using Green Phosphorescent Emitters:

The stack of organic semiconductor films between two electrodes that constitutes an OLED has an electrical capacitance. Moreover, the electron and hole energy levels between adjacent organic layers are often not aligned, which leads to the accumulation of charge at these interfaces that can affect the CV behavior. Since the mobility of holes in most organic materials is higher than that of electrons, holes will preferentially reach various organic/organic interfaces below a certain applied voltage. This accumulation of holes plays a dominant role in the CV behavior of an OLED. Improved charge balance and charge transport kinetics can modify the CV behavior of a device and possibly reduce capacitance.

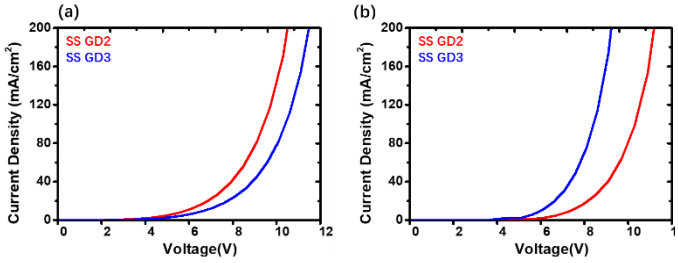

Figure 5. J-V curves of (a) HOD and (b) EOD of the emitter layers in SS GD2 and SS GD3.

We designed another green phosphorescent emitter, SS GD3 with a shallower HOMO level of -5.085 eV (Table 4). The spectrum of SS GD3 is close to that of SS GD2, as shown in Figure 3. Detailed values of λ_{max}, FWHM and shoulder peak intensity of SS GD3 are listed in Table 2. Hole-Only and Electron-Only Devices (HOD and EOD, respectively) were fabricated using both GDs. From the current density-voltage (J-V) curves of the HOD and EOD (Figures 5a-5b), we determined the voltage at a current density of 50 mA/cm^2 (V_{J50}) as a figure of merit (FOM) to study the transport property of the material. For SS GD2 and 3, the V_{J50} values for HOD were 8.2 V and 8.8 V, respectively, while for EOD, they were 9.3 V and 8.9 V, respectively (Table 4). These results indicate that SS GD3 exhibits slower hole transport and faster electron transport compared to SS GD2, leading to a more balanced hole-electron ratio in the device.

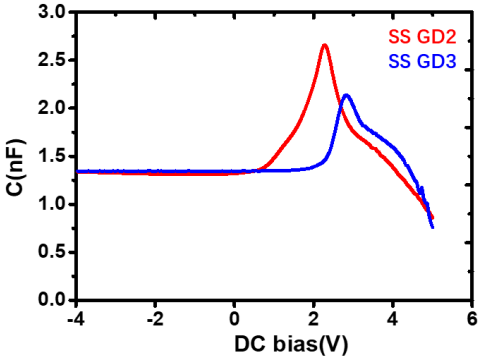

Figure 6. Capacitance vs. voltage (CV) characteristics of bottom-emission devices using SS GDs2 and 3.

We then fabricated bottom-emission devices to characterize the capacitance of SS GD2 and 3 (Figure 6). The CV characteristics were measured at 500 Hz using an Impedance Analyzer (E4990A, Keysight) with an oscillating amplitude of 100 mV. Two FOMs were extracted here to analyze the device characteristics. First, μ-C_{max} is the maximum capacitance extracted from the CV curve divided by the active area of the device (0.04 cm^2), and μ-Q is the total integrated charge minus the charge contributed by the geometric capacitance (C_{geo}) divided by the active area of the device. The total integrated charge is the integral of the capacitances with respect to voltage from -1 V to V_{Cmax}. The charge contributed by the geometric capacitance is the geometric capacitance multiplied by the voltage range. Compared to μ-C_{max}, μ-Q allows for a more comprehensive assessment of how capacitance varies across different voltage levels, providing more information on the charge accumulation inside the device. The capacitance data are summarized in Table 4. The results indicate that the μ-C_{max} and μ-Q of SS GD3 are reduced by 16% and 52%, respectively, compared to SS GD2. The charge accumulation is significantly suppressed, implying an improved charge balance. In addition, the EQE of SS GD3 in bottom-emission devices shows a significant improvement of 6.3% compared to SS GD2 (Table 2). The performance of the top-emission device using SS GD3 is also summarized in Table 3 and the CE vs CIE x curve is plotted in Figure 4. A top-emission OLED with SS GD3 achieved a CE of 230 cd/A, representing a 17% improvement from SS GD2. Therefore, SS GD3 achieves high efficiency as well as low capacitance, meeting the requirements of high-quality displays.

Table 4. Capacitance and charge accumulation properties of SS GD2 and SS GD3, including HOMO energy levels, maximum capacitance (μ-C_{max}), and charge density (μ-Q).

GD	HOMO (eV)	HOD-V_{J50} (V)	EOD-V_{J50} (V)	μ-C_{max} (nF/cm²)	μ-Q (nC/cm²)
SS GD2	-5.123	8.2	9.3	62.5	15
SS GD3	-5.085	8.8	8.9	52.5	7

Green Phosphorescent Emitter for Adobe and BT.2020:

By applying the above strategy, we further designed narrow-spectrum, low-capacitance green phosphorescent emitters (SS GD4–7) for both Adobe RGB and BT.2020 color standards. The EL spectra of SS GD4–7 are displayed in Figure 6a. In particular, SS GD4 and 5 have peak wavelengths of 524 nm and 526 nm with

FWHM values of 30.2 nm and 27.6 nm, respectively, meeting the requirements of the Adobe RGB color gamut. On the other hand, SS GD6 and 7 have peak wavelengths of 522 nm and 518 nm, with FWHM values of 26.9 nm and 27.1 nm, respectively, achieving the BT.2020 color standard.

We also fabricated a series of bottom-emission green OLEDs with these emitters and found that SS GD4, SS GD5, and SS GD7 exhibit particularly low μ-C_{max} and μ-Q (Figure 6b). In particular, SS GD7 exhibits a μ-C_{max} of 49.3 nF/cm^2 and a μ-Q of 5 nC/cm^2. The top-emission device using SS GD5 achieved a high current efficiency of 210 cd/A at 10 mA/cm², with Adobe chromaticity of (0.190, 0.756), a driving voltage of 3.7 V, and LT_{95} exceeding 1,200 hours. The top-emission device using SS GD6 achieved high current efficiency of 182 cd/A at 10 mA/cm², with CIE coordinates of (0.160, 0.779), a driving voltage of 3.4 V, and LT_{95} exceeding 1,100 hours. Due to the deeper HOMO energy level of SS GD6 at -5.209 eV, it exhibits relatively higher capacitance. We are also planning to modify its molecular structure to reduce capacitance while maintaining its high efficiency and balanced charge transport properties. These results highlight the exceptional performance of the SS GD series in terms of efficiency, chromaticity range, and low capacitance, making them highly suitable for advanced display applications.

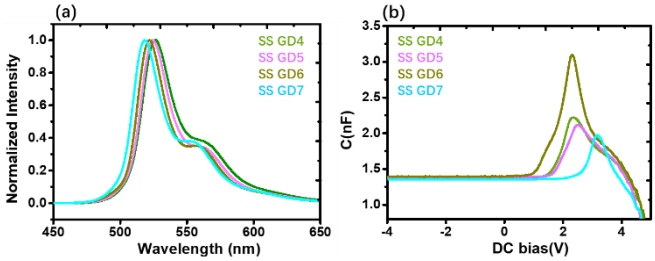

Figure 6. The (a) EL spectral and (b) Capacitance vs. voltage characteristics of SS GD4-7

4. Conclusions and Outlook

In this work, we demonstrated the successful development of a series of green phosphorescent emitters with optimized optical and electrical properties for high-performance OLED displays. By narrowing the spectral FWHM and reducing the shoulder peak intensity, we achieved a significant improvement in efficiency, with SS GD2 showing a 12% increase in efficiency compared to that of SS GD1. Additionally, the chromaticity coordinates of SS GD2 exhibited a blue shift to (0.215, 0.747). Through molecular design, we further developed SS GD3, which features a shallower HOMO energy level and more balanced charge transport properties, leading to a 17% improvement in efficiency and a 16% reduction in capacitance compared to SS GD2. Furthermore, using the same strategy, we designed narrow-spectrum, low-capacitance green phosphorescent emitters (SS GD4–7) for both Adobe and BT.2020 color gamut. The effectiveness of our strategy is validated by the consistent performance improvements demonstrated across the SS GD series.

5. References

1. Gunther H., Microdisplays for augmented and virtual reality. SID Int Symp Dig Tech Pap. 2018;49(1):506-509. https://doi.org/10.1002/sdtp.12445
2. Wang J., Xie M., Pang H., Zhang C., Sang M., Zhang Q., High performance red and green phosphorescent emitters suitable for the BT.2020 color gamut. J Soc Inf Display. 2023;31(6):457-465. https://doi.org/10.1002/jsid.1205
3. Xu Y., Li C., Li Z., Wang J., Xue J., Wang Q., Highly efficient electroluminescent materials with high color purity based on strong acceptor attachment onto B–N-containing multiple resonance frameworks. CCS Chem. 2022;4:2065-2079.
4. Lee J., Park J., Kim Y., Lee H., Kim S., Choi J., Ultrahigh resolution and color gamut with scattering-reducing transmissive pixels. Nat Commun. 2019;10:4782. https://doi.org/10.1038/s41467-019-12689-2.
5. Wang X., Zhang Y., Dai H., Li G., Liu M., Meng G., Mesityl-functionalized multi-resonance organoboron delayed fluorescent frameworks with wide-range color tunability for narrowband OLEDs. Angew Chem Int Ed. 2022; 61:e202206916. https://doi.org/10.1002/anie.202206916
6. Cai X., Xue J., Li C., Liang B., Ying A., Tan Y., Gong S., Wang Y., Achieving 37.1% green electroluminescent efficiency and 0.09 eV full width at half maximum based on a ternary boron-oxygen-nitrogen embedded polycyclic aromatic system. Angew Chem Int Ed. 2022;134:e202200337. https://doi.org/10.1002/anie.202206916
7. Zhang X., Liu X., Sun H., Wu Y., Wan S., Li X., Liu T., Wang D., A high performance full-fluorescent electroluminescent solution with a 96.5% coverage of BT.2020 color gamut. SID Int Symp Dig Tech Pap. 2022;53(1):573-576. https://doi.org/10.1002/sdtp.15552
8. Engelhart J, Stolz S, Ganss S, Ricks M., Materials to enable future OLED display evolution. Information Display. 2023;39(1):6-11.
9. Zhao X., Zhang X., Zhao W., Xu J., Wang H., Song W., The effect of OLED device capacitance on low gray levels motion blur. SID Int Symp Dig Tech Pap. 2024;55:539-541. https://doi.org/10.1002/sdtp.17133
10. Zhao X., Zhang X., Zhao W., Xu J., Wang H., Song W., (2024). 62-3: The effect of oled device capacitance on low gray levels motion blur. SID Symposium Digest of Technical Papers, 55(1).